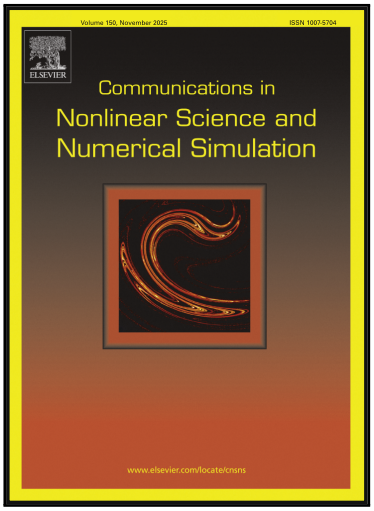

Multiparametric Machine Learning for Predicting Epileptic Hyperexcitability from Interitcal EEG Background Activity

Anton E. Malkov, Albina V. Lebedeva, Svetlana A. Gerasimova, Tatiana A. Levanova, Lev A. Smirnov, Artem A. Sharkov, Alexander N. Pisarchik

PII: S1007-5704(25)00621-5
DOI: https://doi.org/10.1016/j.cnsns.2025.109210
Reference: CNSNS 109210

To appear in: *Communications in Nonlinear Science and Numerical Simulation*

Received date: 2 May 2025
Revised date: 31 July 2025
Accepted date: 8 August 2025

Please cite this article as: Anton E. Malkov, Albina V. Lebedeva, Svetlana A. Gerasimova, Tatiana A. Levanova, Lev A. Smirnov, Artem A. Sharkov, Alexander N. Pisarchik, Multiparametric Machine Learning for Predicting Epileptic Hyperexcitability from Interitcal EEG Background Activity, *Communications in Nonlinear Science and Numerical Simulation* (2025), doi: https://doi.org/10.1016/j.cnsns.2025.109210

Highlights

- Proposes a multiparametric machine learning framework for automated analysis of scalp EEG in epilepsy diagnosis.
- Integrates spectral features, coherence, lateralization, phase-amplitude coupling, and frequency ratios to capture subtle rhythmopathies.
- Focuses on background EEG activity, enabling diagnosis even in the absence of ictal or interictal discharges.
- Successfully clusters epileptic patients into distinct subtypes and achieves high classification accuracy.
- Demonstrates superior performance over conventional EEG analysis methods, supporting clinical decision-making.

Multiparametric Machine Learning for Predicting Epileptic Hyperexcitability from Interitcal EEG Background Activity

Anton E. Malkov[a,b], Albina V. Lebedeva[b,c], Svetlana A. Gerasimova[b], Tatiana A. Levanova[b], Lev A. Smirnov[b], Artem A. Sharkov[b,d], Alexander N. Pisarchik[e,*]

[a] *Institute of Theoretical and Experimental Biophysics, Russian Academy of Sciences, Institutskaya Str., 3, Pushchino, 142290, Moscow region, Russia*
[b] *Lobachevsky State University of Nizhny Novgorod, Gagarin Av., 23, Nizhny Novgorod, 603022, Russia*
[c] *Privolzhsky Research Medical University, Minin and Pozharsky Sq., 10/1, Nizhny Novgorod, 603005, Russia*
[d] *Veltischev Research and Clinical Institute for Pediatrics and Pediatric Surgery, Pirogov Russian National Research Medical University, Taldomskaya Str., 2, Moscow, 125412, Russia*
[e] *Center for Biomedical Technology, Universidad Politécnica de Madrid, Campus de Montegancedo, Pozuelo de Alarcón, 28223, Madrid, Spain*

Abstract

Accurate diagnosis of epilepsy relies on detecting ictal and interictal hypersynchronous activity, yet much of the valuable rhythmic information in EEG recordings remains underutilized. While prolonged EEG monitoring is often required, disruptions in excitatory and inhibitory neurotransmission leading to neural network reorganization can result in rhythmopathy, a disturbance in brain oscillatory rhythms linked to cognitive dysfunction. Analyzing background EEG activity, even in the absence of overt epileptiform discharges, could significantly improve diagnostic accuracy and inform treatment strategies, particularly when clinical recordings fail to capture ictal or interictal events. In this paper, we propose a multiparametric machine learning framework for analyzing scalp EEG recordings in epileptic patients. Our approach incorporates spectral analysis, lateralization coefficients, coherence measures, phase-amplitude coupling, and high-to-low frequency oscillation ratios across key EEG channels. This method enables clustering of patients into distinct diagnostic categories and achieves reliable classification accuracy in distinguishing epilepsy presence. Comparisons with existing techniques demonstrate the superior efficiency of our model. Our findings highlight the potential of automated EEG analysis to assist clinicians in diagnosing epilepsy more rapidly and accurately, ultimately improving patient outcomes.

Keywords: epilepsy, electroencephalography (EEG), machine learning, prediction, rhythmic activity, diagnosis

1. Introduction

Since the seminal work of Fischer and Lowenbach in 1934 [1], which first described the "epileptic spike" as a transient electrographic marker of epilepsy, electroencephalography

*Corresponding author
Email address: alexander.pisarchik@upm.es (Alexander N. Pisarchik)

(EEG) has become a cornerstone in the diagnosis and monitoring of epilepsy. Their research demonstrated that specific patterns of brain activity could be linked to epileptic events, laying the foundation for the use of EEG in clinical practice to not only detect seizures but also to evaluate the efficacy of therapeutic interventions.

In the decades since, EEG has remained an indispensable tool for clinicians, offering critical insights into the electrical activity of the brain. More recently, there has been substantial progress in the development of automatic detection of epilepsy from EEG recordings [2, 3, 4].

These advancements, driven by machine learning (ML) and data analysis techniques, have significantly enhanced the accuracy and efficiency of detecting epileptic activity, paving the way for more reliable and scalable diagnostic tools.

Scalp EEG is a widely used tool for analyzing brain activity during epileptic seizures, leveraging both interictal and ictal phases. The interictal phase represents the period between seizures, where brain electrical activity is relatively stable but may exhibit abnormal patterns, such as interictal epileptiform discharges (IEDs). In contrast, the ictal phase refers to the period of active seizure onset, characterized by abnormal electrical activity and intense dynamic changes in the EEG, including rhythmic discharges, fast oscillations, and evolving frequency-amplitude patterns that reflect the seizure's progression. Both interictal and ictal EEG recordings are crucial for diagnosing and managing epilepsy. The detection of spontaneous seizures or prominent interictal events remains a primary criterion for epilepsy diagnosis [5]. Even in the absence of overt seizure activity, interictal spikes and slow-wave events are commonly observed in patients with epilepsy [6]. These events are central to identifying epileptogenic activity when ictal data is unavailable.

Previous studies have demonstrated the potential of using background EEG analysis for epilepsy detection, reporting promising classification results with limited feature sets [7, 8]. However, many of these approaches were based on EEG data that likely included interictal epileptiform discharges (IEDs), such as spikes and sharp waves, transient events that can strongly influence spectral features and artificially enhance the separability between epileptic and healthy brain activity. While the presence of IEDs, even in short recordings, can boost classification performance, their absence in routine clinical EEGs is common, particularly in brief or resting-state acquisitions. This raises concerns about the generalizability of existing models to real-world diagnostic scenarios where no overt epileptiform activity is present.

To address this limitation, we propose a multiparametric ML framework for classifying temporal lobe epilepsy (TLE) based exclusively on IED-free background EEG activity, excluding both ictal events and interictal discharges. Our approach integrates a comprehensive set of neurophysiological features, including spectral power across standard frequency bands, phase-amplitude coupling (PAC), inter-channel coherence, and spatial asymmetries in background rhythms. By focusing on sustained oscillatory patterns rather than transient abnormalities, we aim to detect subtle, persistent alterations in brain dynamics associated with epileptic pathology.

This work advances the field by shifting the diagnostic focus from episodic biomarkers to intrinsic background rhythm disturbances, which may reflect underlying network dysfunction even in the absence of visible spikes. The proposed method holds promise for enabling rapid, non-invasive detection of epilepsy using short, routine EEG recordings, such as those employed in occupational health screenings or primary care settings, where prolonged monitoring for IEDs is impractical. By validating our model under these more challenging and

clinically representative conditions, we provide a more robust assessment of its potential for real-world deployment.

The remainder of this paper is organized as follows. Section 2 presents an overview of epileptic activity and details the neurophysiological parameters, such as spectral power, functional connectivity, and cross-frequency coupling, used for classification. Section 3 describes the EEG data collection process, including dataset sources and participant characteristics, followed by the preprocessing pipeline, feature extraction methods, and ML framework. Section 4 reports the experimental results, evaluates model performance using subject-wise cross-validation, and provides a comprehensive discussion of the findings in comparison with existing approaches. Finally, Section 5 summarizes the key conclusions, highlights the clinical implications of the study, and suggests directions for future research.

2. Epileptic Activity and Parameters Used

2.1. Epileptic Activity

Epileptic activity is classically defined by the presence of IEDs, including interictal spikes, sharp waves, and associated slow-wave components. These transient EEG phenomena are critical biomarkers in the clinical diagnosis and localization of epilepsy, reflecting abnormal neuronal synchronization in hyperexcitable brain networks.

Interictal spikes (ISs) are brief, high-amplitude deflections lasting up to 100 ms, often occurring in isolation or as part of more complex patterns such as spike-and-wave complexes, polyspikes, sharp-and-slow wave complexes, or periodic discharges [9]. Morphologically distinct from background activity, IEDs are typically focal and may be accompanied by regional slowing. However, their detection poses significant challenges. While high amplitude might seem advantageous for automated identification, non-neural artifacts, such as those from eye movements, muscle activity, or electrode noise, often mimic or obscure true epileptiform signals. As a result, accurate detection requires careful morphological and temporal analysis, traditionally performed by trained epileptologists, making the process labor-intensive and subject to inter-rater variability.

Notably, the sensitivity of IED detection is limited: only a small proportion of individuals following a first unprovoked seizure go on to develop epilepsy with clearly identifiable interictal abnormalities [10]. Conversely, misdiagnosis remains a significant concern, with up to 25% of patients labeled as having epilepsy in developed countries ultimately found not to have the disorder upon re-evaluation [11, 12]. These diagnostic inaccuracies highlight the limitations of relying solely on transient epileptiform events, especially in brief or routine EEG recordings where IEDs may be absent or infrequent.

Moreover, IEDs occupy only a small fraction of a typical EEG recording. The vast majority of the signal consists of ongoing background activity, which is often dismissed as non-informative in routine clinical practice. Yet, growing evidence suggests that the epileptic brain exhibits persistent network-level alterations that extend beyond episodic discharges. Theories of epileptogenesis emphasize structural and functional reorganization of neural circuits, including synaptic remodeling, inhibitory-excitatory (E/I) imbalance, and altered oscillatory dynamics, all of which may manifest as subtle but measurable changes in background EEG rhythms [13].

One such alteration involves high-frequency oscillations (HFOs), particularly ripples (80–250 Hz) and fast ripples (> 250 Hz), which have been shown to colocalize with the seizure onset zone. Bragin et al. [14] demonstrated elevated HFO rates and power in intracranial electrocorticographic (ECoG) recordings from patients undergoing epilepsy surgery, establishing HFOs as potential biomarkers of epileptogenic tissue. However, their detection in scalp EEG is severely limited by low spatial resolution, signal attenuation through skull and tissue, and insufficient sampling rates (typically requiring $\geq$ 1000 Hz) [15], rendering them largely inaccessible in standard clinical settings.

Encouragingly, recent animal and translational studies suggest that HFOs may modulate lower-frequency rhythms, such as 10–16 Hz activity, through cross-frequency coupling or network entrainment. These downstream effects could manifest as detectable shifts in spectral power, coherence, or PAC in scalp EEG, offering a non-invasive window into underlying epileptogenic processes.

Collectively, these insights underscore the importance of moving beyond transient epileptiform events and systematically analyzing the background EEG, a rich, underutilized source of neurophysiological information. By identifying persistent, rhythm-based abnormalities associated with epilepsy, even in the absence of visible spikes, we can develop more robust, generalizable diagnostic tools. This shift is particularly critical for improving detection in short, routine EEGs where prolonged monitoring for IEDs is not feasible, thereby enhancing diagnostic accuracy and reducing misclassification rates.

2.2. Epilepsy Parameters

To comprehensively characterize epilepsy in this study, we analyze a multiparametric set of neurophysiological features derived from scalp EEG. These parameters reflect key aspects of neural network dysfunction in epilepsy: spanning spectral dynamics, cross-frequency interactions, and functional connectivity. They are selected for their sensitivity to underlying pathophysiology, even in the absence of overt epileptiform discharges.

2.2.1. Power Spectral Density (PSD)

The generation and maintenance of rhythmic brain activity rely on a precise balance between excitatory (glutamatergic) and inhibitory (GABAergic) neurotransmission. In epilepsy, this equilibrium is disrupted due to selective loss of inhibitory interneurons and enhanced excitatory signaling [16], leading to aberrant oscillatory activity that can be quantified through PSD analysis of background EEG.

Alterations in spectral power across frequency bands have been consistently linked to epileptogenic processes. For instance, increased delta (1–4 Hz) and theta (4–8 Hz) power, particularly in focal regions, has been associated with seizure onset zones and interictal network dysfunction [17, 18]. Conversely, changes in higher-frequency bands are also informative: reduced gamma (30–100 Hz) variability correlates with cortical dysplasia and poor treatment response [19, 20], while elevated gamma power may reflect local hyperexcitability [21]. Alpha band (8–13 Hz) asymmetries have further been shown to lateralize TLE, supporting their diagnostic value [22].

Spectral asymmetry between hemispheres, especially in theta and delta bands, serves as an additional marker of network imbalance. Li et al. [18] demonstrated significant interhemispheric power differences in TLE patients, while Kalamangalam et al. [23] successfully

used spectral metrics to identify the epileptogenic hemisphere. Moreover, the slope of the power spectrum in the 30–50 Hz range has been proposed as a non-invasive proxy for the cortical E/I ratio, which is known to increase in epileptic tissue [24].

Collectively, PSD provides a robust and interpretable measure of neural population dynamics. Its utility in epilepsy classification has been validated in prior machine learning studies; for example, Kerr et al. [25] employed multilayer perceptrons on multiscale spectral features to distinguish epileptic from healthy EEG with high accuracy, underscoring the diagnostic potential of background rhythm analysis.

2.2.2. Phase-Amplitude Cross-Frequency Coupling

Beyond power, the functional organization of brain rhythms is critically altered in epilepsy. PAC is a form of cross-frequency interaction in which the amplitude of fast oscillations (e.g., gamma) is modulated by the phase of slower rhythms (e.g., delta, theta, or alpha). PAC plays a key role in neural communication and information transfer. Disruptions in PAC are increasingly recognized as hallmarks of epileptogenic networks.

In focal epilepsy, enhanced theta-gamma and delta-gamma PAC has been observed in and around the seizure onset zone, reflecting pathological synchronization and hyperexcitability [26, 27]. These coupling patterns not only help localize epileptogenic foci but also exhibit dynamic changes in the preictal period, suggesting predictive utility for seizure forecasting [28, 29].

Although traditionally studied using intracranial EEG, recent advances confirm that PAC can be reliably assessed in scalp recordings. Grigorovsky et al. [30] demonstrated that scalp-derived PAC captures neural dynamics during postictal suppression, validating its sensitivity to clinically relevant states. Despite its strong pathophysiological basis and diagnostic potential, PAC remains underutilized in routine clinical EEG interpretation. Integrating PAC into automated analysis pipelines could significantly enhance the detection of subtle network abnormalities, particularly in patients without visible interictal spikes.

2.2.3. Coherence and Functional Connectivity

Epilepsy is fundamentally a disorder of network synchronization. Abnormal functional connectivity, manifesting as either excessive local synchronization or impaired long-range communication, underlies both seizure generation and associated cognitive deficits [31].

EEG coherence, a measure of linear synchronization between signals from different brain regions, reveals complex alterations in epilepsy. Elkholy et al. [32] reported reduced resting-state coherence in delta and theta bands, accompanied by increased phase lag, which correlated with interictal discharge frequency. Paradoxically, other studies have observed elevated coherence in specific frequency bands, suggesting a state of maladaptive over-synchronization within epileptic networks [33].

Notably, coherence patterns may also reflect treatment response. Drug-resistant patients often exhibit heightened gamma-band coherence, possibly indicating persistent pathological network coupling [34]. Conversely, antiseizure medications such as topiramate have been shown to normalize excessive coherence in lower frequencies, aligning with clinical improvement.

Despite inter-study variability, attributable to differences in patient populations, recording conditions, and analytical methods, coherence and related connectivity metrics (e.g.,

phase-locking value, Granger causality) remain valuable tools for mapping epileptic networks and improving focus localization [35, 36]. When combined with spectral and cross-frequency features, they contribute to a more holistic assessment of brain dynamics in epilepsy.

3. Data and Methods

3.1. EEG Data

We analyzed datasets of 33 adult patients from publicly available sources, including Physionet, OpenNeuro, and the American University of Beirut, which comprised both epilepsy patients and healthy controls from the following databases:

1. Siena scalp EEG database: 14 patients (9 males, aged 25–71, and 5 females, aged 20–58).

2. Verbal working memory epilepsy dataset: 15 patients (7 males, aged 19–47, and 8 females, aged 18–56).

3. American University of Beirut epilepsy EEG database: 4 patients (2 males, aged 22 and 24, and 2 females, aged 12 and 14).

The diagnosis and seizure classification for each patient were conducted by a clinical expert, following the guidelines of the International League Against Epilepsy (ILAE). Each case involved a detailed review of both clinical and electrophysiological data.

For the control group, we utilized EEG recordings from sex-matched, healthy adults from the American University of Beirut, as well as datasets from OpenNeuro [A Resting-State EEG Dataset for Sleep Deprivation; `http://dx.doi.org/10.18112/openneuro.ds004902.v1.0.5`] and Physionet [EEG During Mental Arithmetic Tasks, `http://dx.doi.org/10.13026/C2JQ1P`]. Only resting-state EEG recordings were included in the analysis.

All EEG data were resampled to 500 Hz and filtered using a bandpass of 0.5–200 Hz. A 50-Hz notch filter was applied when necessary to eliminate powerline interference. For the epileptic recordings, interictal activity and artifacts were removed using amplitude-based filters. Seizure events, as well as data within 30 minutes before and after seizures, were excluded in accordance with seizure prediction time horizons from EEG features [37]. A total of twenty standard EEG leads were utilized for the analysis: Fp1, Fp2, F3, F4, F7, F8, C3, C4, T3, T4, P3, P4, T5, T6, O1, O2, Fz, Cz, Oz, and Pz.

Figure 1(a) illustrates the raw EEG signals from 60-second trials recorded from the F3 channel for both a healthy control participant and an epileptic patient.

The cleaned EEG data were segmented into 1-minute epochs, yielding 2,346 epochs from epilepsy patients who exhibited no seizure or interictal discharges, and 1,151 epochs from healthy controls.

Data analysis was conducted using Igor Pro 6.32 (WaveMetrics) and Python packages, ensuring robust and replicable processing techniques for EEG signal examination.

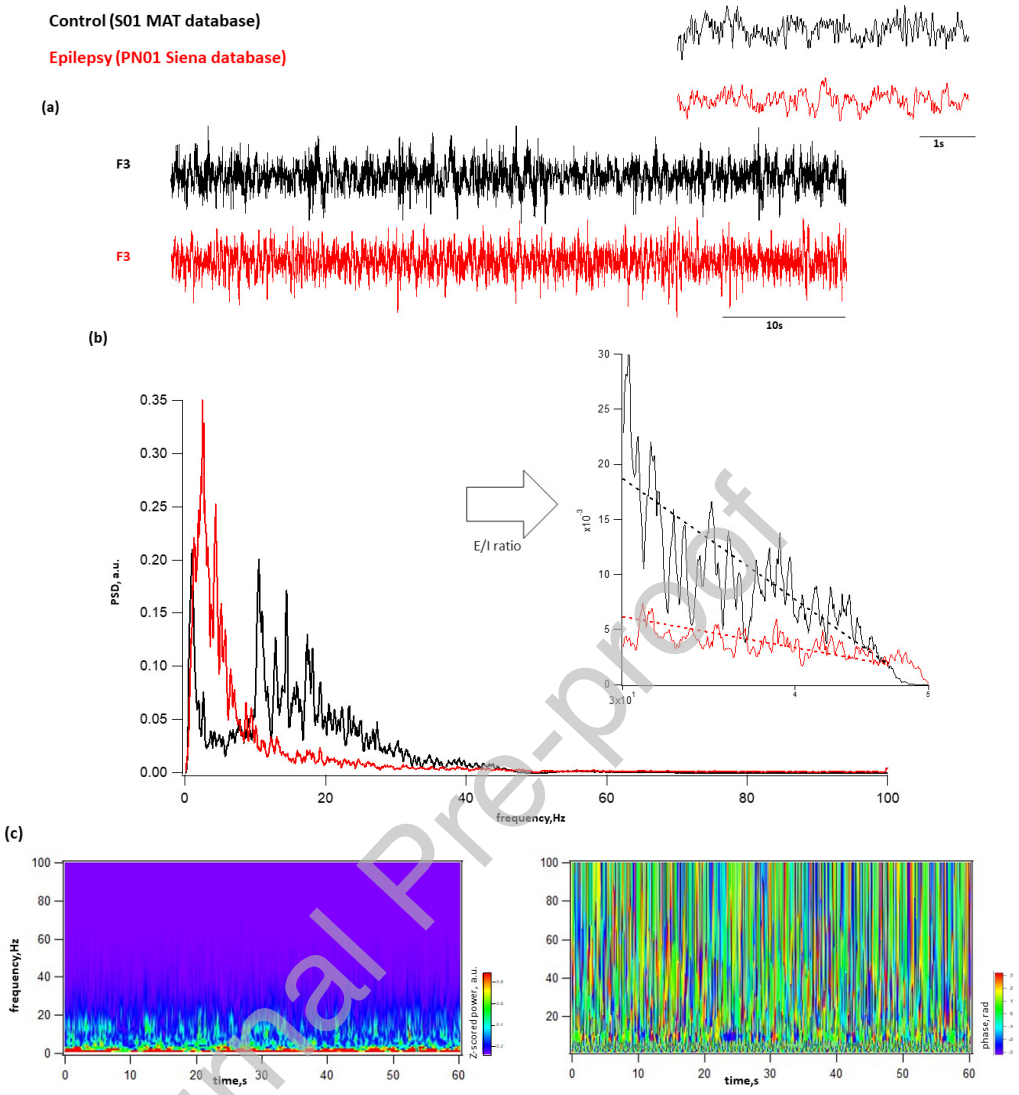

Figure 1: Overview of the analysis pipeline and representative examples of two epochs from the F3 lead of an epileptic patient (red) and a healthy individual (black). (a) Raw 60-second signal epochs for a healthy subject (black) and an epileptic patient (red) and cleaned 5-second trials (top right). (b) Power spectrograms illustrating the frequency content over time. The inset displays the linear approximation of the spectrum in the 30–50 Hz range, which is used for calculating the E/I ratio. (c) Result of wavelet transformation followed by the calculation of oscillation phases.

3.2. Feature Extraction

PSD was estimated for each channel and epoch using Welch's method, with non-overlapping segments (Fig. 1(b)). For each epoch, the integrated power was computed across the following frequency bands: delta (1–4 Hz), theta (4–8 Hz), alpha (8–13 Hz), beta (13–30 Hz), and gamma (30–100 Hz). This produced a time-varying profile of band power for each frequency, with each data point representing the average power within a 60-second window. To ensure consistent scaling, the band power values were log-transformed and standardized across all epochs and channels for each frequency band.

Lateralization coefficients were calculated to assess hemispheric asymmetry in power

spectral density. These coefficients were defined as the ratio of the PSD in the left hemisphere (PSDL) to that in the right hemisphere (PSDR) for frontal (F3/F4), central (C3/C4), and parietal (P3/P4) electrodes. Given that the epileptic focus could vary between hemispheres, the absolute lateralization was quantified using the following formula:

$$L = \left| \frac{\text{PSDL}}{\text{PSDR}} - 1 \right|. \tag{1}$$

This measure provided an indicator of inter-hemispheric power asymmetry in each frequency band.

Additionally, total power was computed for frontal, central, and parieto-occipital regions to further characterize the spatial distribution of neural activity.

The E/I ratio was estimated using the approach proposed by Gao et al. [24]. This involved calculating the log-transformed PSD slope in the 30–70 Hz range, where a steeper and more negative slope is indicative of greater inhibitory activity (Fig. 1(b)).

3.3. Phase-Amplitude Coupling (PAC)

Wavelet transforms were employed to analyze the phase and amplitude of oscillations, as illustrated in Fig. 1(c) and Fig. 2. For each frequency (1–100 Hz, in 1-Hz increments), high-amplitude components exceeding three standard deviations were identified. The integrated amplitude of these selected components was then normalized for each frequency, enabling the construction of cross-frequency and phase-amplitude diagrams. The modulation index, which quantifies the coupling between high-frequency amplitudes and low-frequency phases, was calculated using the Kullback-Leibler distance; higher values indicate stronger coupling.

Preliminary analyses revealed that theta-gamma and delta-gamma couplings were the most pronounced, and these were prioritized for further investigation. In addition to data from individual electrodes, we also calculated regional parameters as the average of neighboring leads: F3 + F4 + Fz for the frontal region, C3 + C4 + Cz for the central region, P3 + P4 + Pz for the parietal region, and T3 + T4 + T5 + T6 and O1 + O2 + Oz for the temporal and occipital regions, respectively.

3.4. Phase Coherence

Phase coherence was evaluated by calculating the phase differences between corresponding rhythms across all leads, emphasizing both global coherence (the average phase difference relative to the Cz lead) and interhemispheric coherence (the phase differences between electrode pairs F3-F4, C3-C4, P3-P4, and T3-T4). Coherence was defined as the probabilistic distribution of phase differences, with a maximum coherence value of 1 indicating perfect synchronization (Fig. 3).

3.5. Statistical Analysis

To evaluate differences in features between the control and epilepsy groups, we performed two-sample t-tests for each feature. To account for the risk of false positives due to multiple comparisons, we applied a Bonferroni correction. Features with corrected $p \leq 0.01$ were considered highly significant.

(a)

(b)

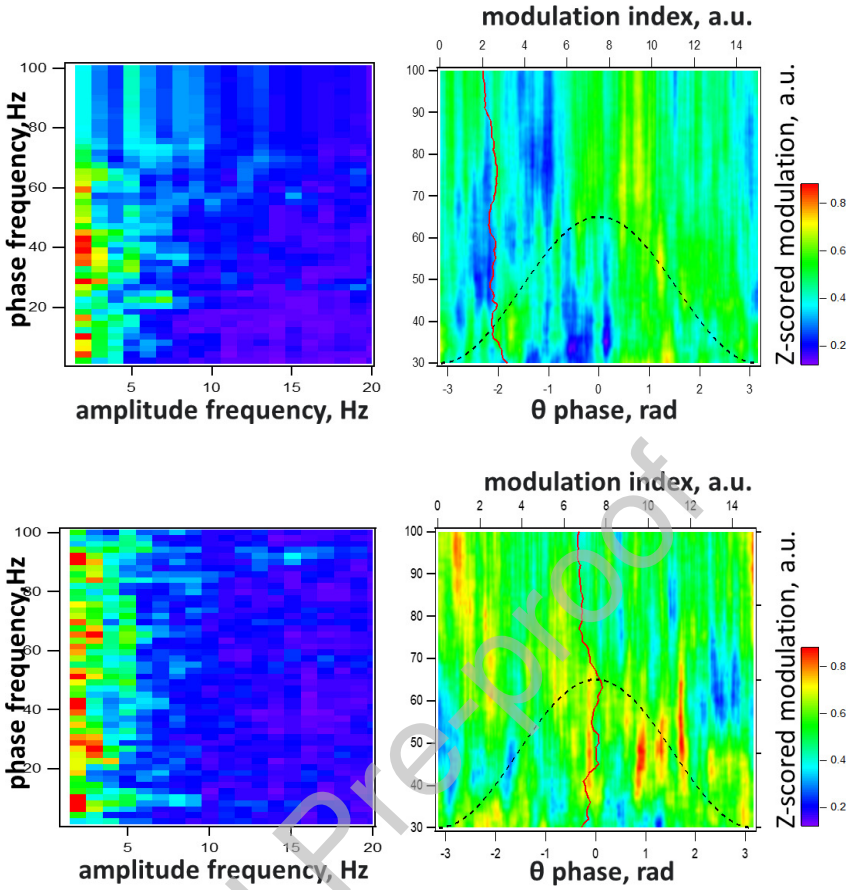

Figure 2: Cross-frequency (left panels) and phase-amplitude (right panels) diagrams of the Z-scored modulation index (indicated by color) for (a) control group and (b) epileptic patients, for trials presented in Fig. 1. The red dashed lines show the modulation index profile for gamma frequencies.

3.6. Machine Learning Methods

We employed ML techniques to classify samples based on 3,497 epochs, each described by 258 features. To reduce the dataset's dimensionality while preserving variance, principal component analysis (PCA) was applied, retaining 95% of the total variance. PCA transforms standardized features into orthogonal components, reducing computational complexity and improving generalization by focusing on the most informative aspects of the data.

We utilized four ML algorithms for classification: logistic regression (LR), support vector machines (SVM), random forest (RF), and gradient boosting (GB). The analysis workflow included data preprocessing, applying the classification models, and evaluating their performance through metrics such as accuracy, precision, recall, and F1 score. PCA was also incorporated to further reduce complexity and improve the efficiency of the models.

3.7. Data Preprocessing

The dataset, consisting of 258 features per sample and a binary target label ("healthy" or "epileptic"), was split into training and test sets using a 70:30 ratio. Stratified sampling

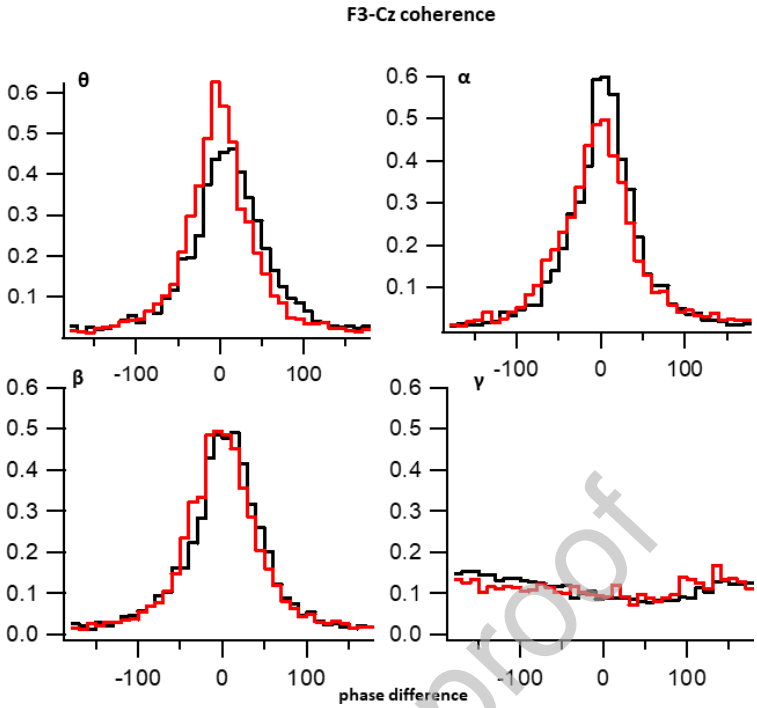

Figure 3: Probability distributions of the phase differences between the F3 and Cz leads across main frequency bands: theta (4–8 Hz), alpha (8–13 Hz), beta (13–30 Hz), and gamma (30–100 Hz), excluding delta (1–4 Hz) due to exceedingly high values. Black – control group, red – epileptic patients.

preserved the original class distribution. All features were standardized using the StandardScaler, ensuring zero mean and unit variance. This step was essential for algorithms sensitive to feature scaling.

3.8. Model Performance Evaluation

To assess classification quality, we used the following evaluation metrics:

- **Accuracy:** the proportion of correctly classified samples:

$$\text{Accuracy} = \frac{TP + TN}{TP + TN + FP + FN}$$

- **Precision:** the proportion of true positives among all predicted positives:

$$\text{Precision} = \frac{TP}{TP + FP}$$

- **Recall (Sensitivity):** the proportion of true positives among all actual positives:

$$\text{Recall} = \frac{TP}{TP + FN}$$

- **F1-Score:** the harmonic mean of precision and recall:

$$\text{F1-score} = 2 \cdot \frac{\text{Precision} \cdot \text{Recall}}{\text{Precision} + \text{Recall}}$$

- **ROC AUC:** the area under the receiver operating characteristic curve, indicating the model's ability to distinguish between classes across various thresholds.

To ensure robust performance estimation and minimize overfitting, we used 5-fold cross-validation. The dataset was split into five subsets (folds); in each iteration, one fold was used for testing and the remaining four for training. The metrics were averaged across all folds to obtain final performance scores.

4. Results and Discussion

In this section, we present the principal findings of our study, supported by empirical observations and quantitative outcomes. For each set of results, we provide a focused discussion that interprets the findings, contextualizes them within the existing literature, and highlights their implications for understanding epilepsy-related EEG dynamics.

4.1. Spectral Power

Spectral power analysis revealed significant differences between epilepsy patients and healthy controls across multiple frequency bands. Slow-wave activity (delta and theta) showed substantial increases in epilepsy patients, especially in frontal leads (Fp1, Fp2, F3, F4, Fz) (Fig. 4(a)). Theta power was also elevated in parietal leads (P4, Pz), suggesting widespread alterations.

Specifically, delta power in frontal regions averaged 0.36 ± 0.08 in epilepsy patients, compared to 0.27 ± 0.07 in controls ($p < 0.01$). Theta power was also elevated in patients, averaging 0.25 ± 0.04 versus 0.21 ± 0.03 in controls ($p < 0.01$). In parietal leads, theta power was 0.253 ± 0.03 in patients compared to 0.17 ± 0.06 in controls ($p < 0.01$).

In contrast, higher-frequency rhythms (alpha, beta, gamma) were significantly reduced in patients with epilepsy compared to controls. Specifically, frontal alpha power was 0.11 ± 0.03 in patients versus 0.14 ± 0.04 in controls ($p < 0.01$), beta power was 0.13 ± 0.07 vs. 0.18 ± 0.06 ($p < 0.01$), and gamma power was 0.065 ± 0.025 vs. 0.095 ± 0.059 ($p < 0.01$).

These findings are consistent with a growing body of evidence indicating that epilepsy is associated with a distinct and reproducible spectral signature in the background EEG [38, 39, 40]. Specifically, elevated power in the delta (1–4 Hz) and theta (4–8 Hz) bands, coupled with reduced activity in the alpha (8–13 Hz) and gamma (30–100 Hz) ranges, reflects widespread disruptions in cortical network dynamics. Such alterations are thought to arise from imbalances in E/I neurotransmission, synaptic reorganization, and impaired thalamocortical regulation – hallmarks of epileptogenic tissue [13, 24].

However, these spectral patterns are not unique to epilepsy. Similar shifts, particularly increased delta and theta power, are commonly observed during non-rapid eye movement (NREM) sleep [41, 42], raising a critical confound: could the observed differences reflect variations in vigilance state rather than underlying pathology? To address this, we ensured that all healthy control participants were in a state of quiet wakefulness during EEG acquisition, with eyes closed or engaged in low-cognitive-load tasks, minimizing the influence of drowsiness or sleep onset.

In contrast, the arousal state of epilepsy patients was less uniformly documented. While recordings from subjects performing verbal working memory tasks (e.g., in the Temple University dataset) can be reasonably assumed to reflect wakefulness, data from the Siena Scalp

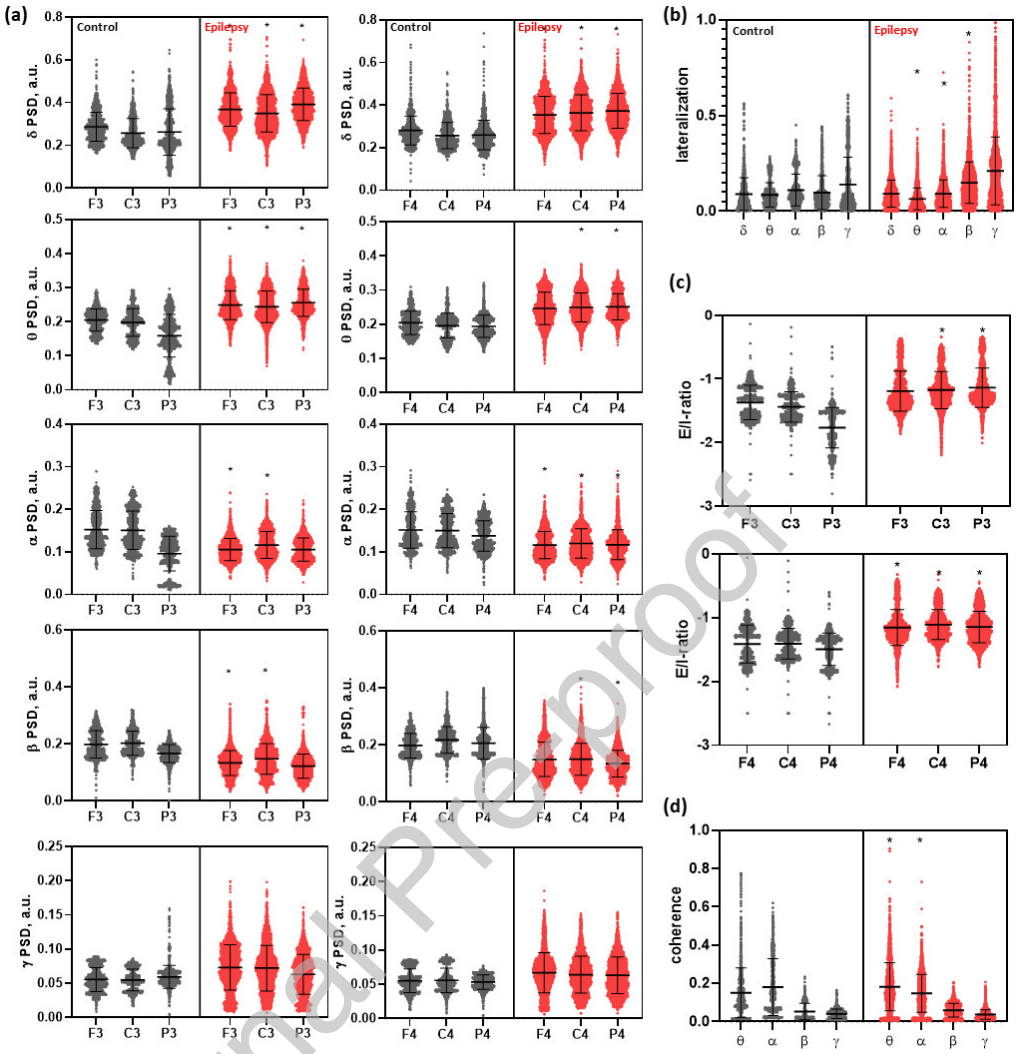

Figure 4: Analysis of background EEG parameters for leads F3, F4, C3, C4, P3, and P4. (a) Power of the primary EEG rhythms: delta (1–4 Hz), theta (4–8 Hz), alpha (8–13 Hz), beta (13–30 Hz), and gamma (30–100 Hz). (b) Lateralization coefficients across frequency bands, reflecting hemispheric asymmetry. (c) Excitation/Inhibition (E/I) ratio coefficients, calculated from the power spectral density slope in the 30–70 Hz range. (d) Average coherence of the main EEG rhythms across all leads. Control group data are displayed in gray, while parameters for epilepsy patients are shown in red. Lines indicate mean and standard deviation (SD). Statistically significant differences between control and epilepsy groups are denoted by *, $p < 0.01$.

EEG Database included mixed sleep-wake recordings without detailed annotations of sleep staging or duration. This constitutes a limitation of the current study.

Despite this uncertainty, several lines of evidence support a pathological rather than state-dependent interpretation of the observed spectral changes. First, the pattern of abnormalities, particularly the pronounced and widespread increase in slow-wave activity and suppression of high-frequency rhythms, exceeds typical variations seen in physiological sleep. Second, the alterations were consistently present across diverse datasets and patient subgroups, suggesting a robust and generalizable effect. Third, prior intracranial and magne-

toencephalography (MEG) studies have localized similar spectral disturbances to epileptogenic zones, independent of sleep state [40, 43], reinforcing their disease-specific nature.

Moreover, the directionality of the changes, reduced gamma power, altered alpha asymmetry, and elevated delta/theta, is consistent with known neurobiological mechanisms in epilepsy, including interneuron loss, synaptic sprouting, and aberrant oscillatory coupling. These features are increasingly recognized as potential biomarkers of epileptogenic networks, even in the absence of interictal spikes.

Importantly, our results suggest that these background rhythm abnormalities carry sufficient discriminative power to significantly enhance the performance of machine learning models for epilepsy detection. By focusing on sustained, state-independent spectral deviations rather than transient events, this approach offers a promising pathway toward more reliable and scalable diagnostic tools, particularly for short, routine EEGs where interictal discharges are often absent.

Future studies should aim to disentangle sleep-related from pathology-driven spectral changes through rigorous sleep staging and longitudinal monitoring. Nonetheless, the consistency and magnitude of the observed effects in this study strongly support the utility of background EEG spectral analysis as a clinically relevant and biologically grounded approach to epilepsy classification.

4.2. Lateralization of Activity

To assess hemispheric lateralization of rhythm power, we calculated an absolute lateralization coefficient, which reflects the degree of asymmetry regardless of which hemisphere was dominant, as defined by Eq. (1).

Our analysis revealed that epilepsy patients exhibited reduced lateralization in the alpha band (0.09 ± 0.06 vs. 0.2 ± 0.09, $p < 0.01$) and theta band (0.065 ± 0.05 vs. 0.10 ± 0.08, $p < 0.01$) compared to healthy controls. However, in the beta band, lateralization was significantly higher in epilepsy patients (0.15 ± 0.1) compared to controls (0.10 ± 0.08, $p < 0.01$) (Fig. 4(a)).

Lateralization of slow rhythms (delta and theta) is commonly used in clinical research to help localize seizure foci [18, 44]. Although our findings do not directly support increased lateralization of slow rhythms in epilepsy, this may be due to the heterogeneity of patient groups and the evaluation methods used. Conversely, the increased beta-band lateralization observed in epilepsy patients could suggest altered cortical network functioning in regions involved in cognitive tasks near the seizure focus compared to the contralateral hemisphere.

4.3. E/I Ratio

The analysis of the E/I ratio, based on the power spectral slope, revealed a significant increase in excitatory neurotransmission in epilepsy patients across all leads (Figs. 1(b) and 4(c)). On average, the PSD slope in the 30–70 Hz range was steeper in epilepsy patients (-1.1 ± 0.23) compared to healthy controls (-1.42 ± 0.25, $p < 0.01$). The most pronounced changes were observed in the Fp1, Pz, P3, and P4 leads.

While this parameter has not been extensively used to characterize EEG in epilepsy, it shows potential for enhancing classification of resting-state activity by providing insights into the balance between excitatory and inhibitory neural activity. The increased E/I ratio observed in epilepsy patients may indicate heightened excitatory activity, which is consistent

with the pathophysiology of epilepsy and could serve as a useful marker for future diagnostic and therapeutic applications.

4.4. Coherence

In our analysis of average coherence across all EEG leads, we found that in healthy individuals, coherence was higher in the alpha band (0.18 ± 0.14) compared to the theta band (0.15 ± 0.12). In contrast, epilepsy patients exhibited increased theta coherence (0.18 ± 0.12) and reduced alpha coherence (0.15 ± 0.09).

The observed increase in theta coherence aligns with findings from previous studies in both animal models of epilepsy [27] and human patients [45, 46].

In healthy brains, increased theta coherence, along with alpha desynchronization, is commonly seen during tasks involving working memory and attention, where it facilitates communication between cortical and subcortical structures. However, the persistent increase in theta coherence observed in epilepsy patients may reflect impaired network control, particularly in the brain's ability to switch between the default mode network and the frontoparietal central executive network [47]. This disruption likely contributes to the cognitive impairments often seen in epilepsy.

4.5. Functional Connectivity

In this study, PAC analysis revealed marked abnormalities in cross-frequency modulation in patients with epilepsy. As illustrated in Fig. 5(a), the modulation index, quantifying the strength of phase-amplitude interactions, exhibited a skewed distribution in the epilepsy group compared to controls. While healthy individuals displayed a broad and dynamic range of modulation, consistent with flexible neural communication across cognitive states, epilepsy patients showed less variability and abnormally elevated coupling in specific frequency pairings, particularly delta-gamma and theta-gamma.

These aberrant PAC patterns suggest a breakdown in the brain's ability to regulate large-scale network interactions. Pathologically enhanced coupling may reflect excessive synchronization within hyperexcitable circuits, potentially promoting seizure generation while impairing normal information processing. Such disruptions are thought to contribute to the cognitive deficits commonly observed in epilepsy, including impaired memory, attention, and executive function [48].

Notably, abnormal PAC has been previously reported in the seizure onset zone and surrounding tissue [26, 28], supporting its role as a biomarker of epileptogenic networks. Our findings extend this observation to scalp EEG, demonstrating that cross-frequency disturbances are detectable even in non-invasive recordings and across diverse patient cohorts. This reinforces the potential of PAC as a sensitive, non-invasive tool for probing functional network pathology in epilepsy, complementing traditional spike-based diagnostics and offering insight into the broader impact of epilepsy on brain dynamics.

4.6. Phase-Amplitude Cross-Frequency Modulation

In epilepsy patients, the integrated modulation index for delta-gamma coupling (DGC) was significantly elevated, with a value of 241 ± 78, compared to 99 ± 65 in healthy individuals. Similarly, the theta-gamma coupling (TGC) was 154 ± 38 in epilepsy patients, while healthy individuals showed a lower value of 174 ± 89.

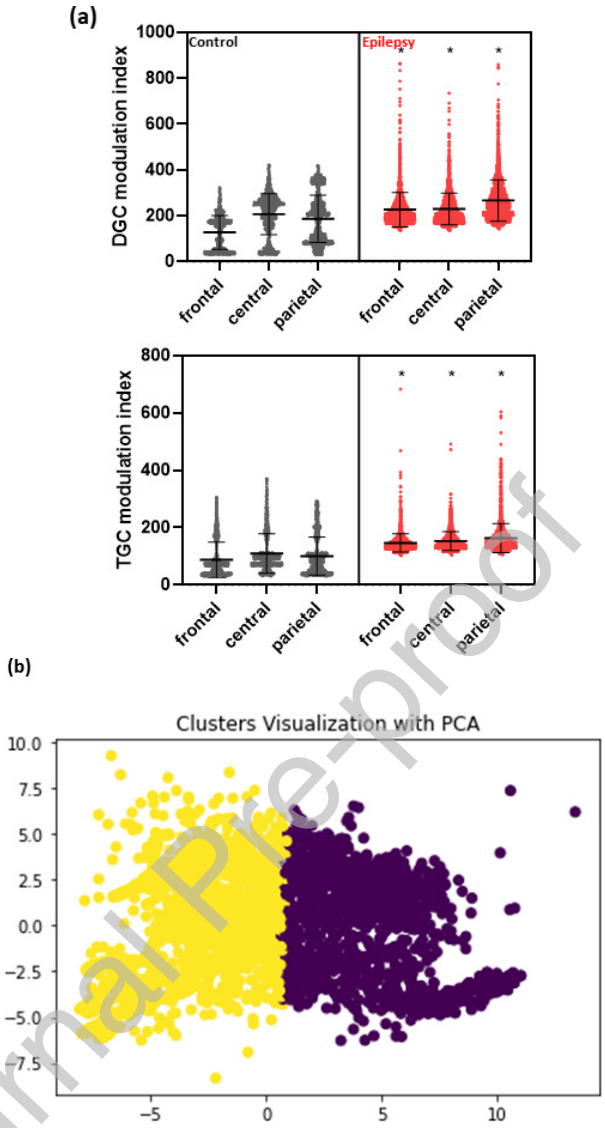

Figure 5: (a) Integrated delta-gamma and theta-gamma modulation indices for frontal, central, and parietal leads in healthy subjects and epilepsy patients. Mean values and standard deviations (SD) are represented by lines. Statistical significance between control and epilepsy groups is denoted by *, $p < 0.01$. (b) Clustering of data into two groups using principal component analysis (PCA), illustrating the separation between control and epilepsy samples.

Despite decreased gamma power, modulation strength increased, reflecting altered temporal structure of neural oscillations. Interestingly, while animal models of epilepsy also show elevated baseline TGC levels, these increases do not consistently correlate with cognitive performance, as seen in control groups [27]. Our findings suggest that the enhanced TGC and DGC could serve as reliable markers for distinguishing pathological brain activity from normal resting-state conditions in humans.

Table 1: Performance Metrics of Machine Learning Models Evaluated in This Study

Model	**CVA**	**Accur**	**Precis**	**Recall**	**F1-score**	**ROC**
LR	0.9997	1	1	1	1	1
SVM	1	1	1	1	1	1
RF	0.9991	0.9990	0.9986	1	0.9992	0.9986
GB	0.9982	0.9971	0.9958	1	0.9979	0.9957

4.7. Clustering and Model Performance

Feature importance was analyzed using a logistic regression model, trained on 700 pre-labeled epochs (263 from controls and 437 from epilepsy patients). The model achieved a perfect prediction rate of 100%, demonstrating the robustness of the selected features. Key distinguishing features included alpha power at FP1, F3, and C4 leads; beta power at P4; theta power at P3; total gamma power across frontal, central, and parietal leads; the E/I ratio at P3, P4, and Pz leads; and the modulation index for delta-gamma coupling at frontal leads.

Principal Component Analysis (PCA) was used to cluster the epochs based on these features. Of the 2,346 epochs from epilepsy patients, 1,351 were correctly identified as pathological. Only 44 out of 1,151 epochs from healthy individuals were incorrectly classified as epileptic (Fig. 5(b)).

The consistent high performance across diverse ML algorithms, including linear (LR), kernel-based (SVM), and ensemble methods (RF, GB), demonstrates the robustness of the extracted features, with all models achieving near-perfect or perfect classification accuracy (Table 1).

It should be noted that the LR and SVM models achieved perfect scores across all metrics, including accuracy (Accur), precision (Precis), recall, F1-score, and ROC analyses, demonstrating flawless classification of samples into control and epilepsy groups. Other models, such as RF and GB, also delivered impressive results, with accuracy rates nearing 100%. Specifically, the RF model achieved an accuracy of 99.90%, while the GB model reached 99.71%. These findings indicate that all methods are highly effective for this specific classification task.

While the 100% accuracy of the LR and SVM models is commendable, it raises concerns about potential overfitting. To ensure the robustness and real-world applicability of these models, it is essential to validate them on completely unseen external datasets that capture natural EEG variability. However, due to the lack of access to independent external EEG datasets, all ML models in this study were trained and evaluated using pooled open-access data. To mitigate the risk of data leakage under these constraints, we implemented a more rigorous subject-wise 5-fold cross-validation, where training and testing splits were performed across different individuals rather than through random shuffling of epochs. Specifically, each fold included data only from patients not seen during training, ensuring that no subject's recordings were present in both training and test sets.

Subject-wise cross-validation is a critical methodological safeguard in EEG-based classification, particularly given the high degree of both inter-subject and intra-subject variability

Table 2: Performance of machine learning models using subject-wise cross-validation

Model	Accur	Precis	Recall	F1-score	ROC
LR	0.9431	0.932	0.9872	0.9588	0.9927
SVM	0.9257	0.9126	0.9834	0.9467	0.9902
RF	0.9297	0.914	0.9881	0.9496	0.9769
GB	0.9162	0.8974	0.9881	0.9406	0.8244

inherent in neurophysiological signals. EEG recordings vary significantly across individuals due to differences in age, neuroanatomy, skull conductivity, brain morphology, electrode placement, and baseline neurophysiological profiles. These inter-subject differences can profoundly influence spectral and connectivity features, potentially leading to overfitting if training and testing data are not strictly separated at the subject level.

In addition, EEG signals from the same individual can change over time due to fluctuations in vigilance, medication effects, disease progression, or neurodevelopmental maturation—factors especially relevant in epilepsy, where brain dynamics evolve across the lifespan. Without proper subject-wise partitioning, models may inadvertently learn subject-specific artifacts or transient states, resulting in inflated performance estimates that do not generalize to new patients.

By ensuring that entire subjects are held out during training and used exclusively for testing, subject-wise cross-validation prevents data leakage and provides a more realistic assessment of a model's ability to generalize to unseen individuals. This is particularly important in clinical translation, where diagnostic tools must perform reliably on new patients with diverse demographic and pathological profiles. As such, subject-wise cross-validation not only strengthens the validity of our results but also aligns our evaluation framework with real-world deployment scenarios, where robustness across individuals is paramount.

The evaluation was performed using features derived from PCA-transformed inputs. The performance metrics of the ML models using subject-wise cross-validation are presented in Table 2.

These results suggest that the models retain strong performance even under stricter cross-validation, with particularly high recall values indicating sensitivity to epileptic patterns. The small performance drop compared to random-split cross-validation is expected and supports the models' robustness and potential applicability in clinical settings. Furthermore, we evaluated the performance of various ML methods using only rhythm power features.

To assess the added value of advanced EEG features, we also trained the models using only traditional rhythm power features. Table 3 shows the results using the same subject-wise cross-validation strategy.

Table 3: Performance of machine learning models using only rhythm power features (subject-wise cross-validation)

Model	Accuracy	Precision	Recall	F1-score	ROC AUC
LR	0.7807	0.8311	0.9228	0.8745	0.7730
SVM	0.8976	0.9359	0.9408	0.9383	0.9397
RF	0.9436	0.9844	0.9469	0.9653	0.9859
GB	0.9243	0.9777	0.9305	0.9978	0.9532

Although high accuracy was also achieved with rhythm power alone, particularly using ensemble models, the inclusion of additional features such as PAC and the E/I ratio led to consistently better results across most metrics. This highlights the advantage of multiparametric EEG analysis in improving the reliability and diagnostic accuracy of classification models.

Finally, compared to previous studies, our model demonstrates superior performance by integrating a broader set of physiological features and relying solely on background EEG activity, without requiring interictal discharges or ictal events. Table 4 represents the comparison of classification performance across different studies which used EEG-based ML for epilepsy detection.

5. Conclusion

This study demonstrates the diagnostic potential of analyzing background EEG rhythms for distinguishing individuals with epilepsy from healthy controls, even in the absence of interictal epileptiform discharges or ictal events. We identified robust and reproducible neurophysiological signatures of epilepsy, characterized by elevated delta and theta power and reduced activity in the alpha, beta, and gamma bands, particularly over frontal and parietal regions. These spectral alterations were consistent across multiple independent datasets, supporting their reliability as markers of underlying epileptogenic network dysfunction.

Beyond spectral power, we observed significant changes in functional brain dynamics. An elevated E/I ratio, estimated from high-frequency spectral slopes, along with disrupted coherence patterns, such as increased theta-band and reduced alpha-band synchronization, reflects widespread abnormalities in cortical network organization. Furthermore, PAC analysis revealed pathological modulation of gamma amplitude by slow delta and theta rhythms, indicating impaired cross-frequency communication, a potential contributor to both seizure generation and cognitive comorbidities.

Using a multiparametric feature set encompassing spectral, connectivity, and cross-frequency metrics, we trained and evaluated multiple ML models: LR, SVM, RF, and GB. All models achieved near-perfect or perfect classification accuracy, with PCA enhancing feature efficiency and generalizability. Critically, subject-wise cross-validation confirmed high sensitivity and robustness across individuals, underscoring the model's ability to generalize to new, unseen subjects, a key requirement for clinical deployment.

Compared to prior studies, our approach advances the field by integrating a broader range of physiologically grounded features and focusing exclusively on background EEG activity, independent of transient epileptiform events. This enables reliable classification even in

Table 4: Comparison of classification performance across studies using EEG-based machine learning for epilepsy detection

Study Source	**ROC**	**Parameters Used**	**Data Source**	**Data Length**	**Methods Used**
Current study	99–100%	PSD, PAC, E/I ratio, coherence	1. Siena Scalp EEG 2. Verbal Working Memory Epilepsy Dataset 3. AUB Epilepsy EEG Database 4. EEG under Sleep Deprivation 5. EEG during Mental Arithmetic Tasks	≈200,000	LR, SVM, RF, GB
[7]	90–96%	Wavelet power	Bonn University "Klinik für Epileptologie"	≈10,000 (20-s segments)	Intracranial EEG; contains IEDs and seizures; MLP, ELMAN
[8]	92–100%	Wavelet power	Bonn University "Klinik für Epileptologie"	≈10,000 (20-s segments)	Intracranial EEG; contains IEDs and seizures; MLP, GRNN, ELMAN, PNN, RBF
[49]	≈80%	Raw signal (no feature extraction)	TUH EEG Corpus	≈160,000	Single bipolar channel; includes IEDs and seizures; CNN+LSTM
[50]	96%	PSD	Restricted database	≈105,000	Epileptic vs. non-epileptic seizures; SVM, kNN, LDA, MLP, CNN
[51]	94%	PSD, neuronal fragility, source-sink metrics	Johns Hopkins, UPMC, NIH, etc. (6 centers)	≈250,000	Multicenter EEG study

short, routine EEG recordings where interictal spikes may be absent, making the method particularly suitable for point-of-care screening and resource-limited settings.

Despite these promising results, several limitations must be acknowledged. First, the models were trained and validated on pooled public datasets, with no access to independent, prospectively collected clinical cohorts. This limits definitive assessment of real-world generalizability. Second, while healthy controls were confirmed to be awake during recordings, vigilance state annotations for epilepsy patients were incomplete, particularly in datasets containing mixed sleep-wake segments, raising the possibility that sleep-related spectral changes could partially confound the results. Third, although interictal discharges may enhance classification performance when present, the true diagnostic utility of background EEG in their absence remains an open question, especially in standard clinical EEGs where such events are often missing.

Future work should focus on validating the model on external, clinically annotated datasets with detailed metadata, including sleep staging, seizure type, and medication status. Improved labeling of interictal activity will help disentangle its contribution from background rhythm abnormalities. Expanding the framework to multi-class classification (e.g., differen-

tiating epilepsy syndromes or focal onset types) and testing under realistic conditions, such as noisy, artifact-contaminated, or ultra-short EEGs, will further enhance clinical relevance. Finally, integrating background rhythm-based classifiers with conventional spike detection pipelines could provide a more comprehensive diagnostic tool, bridging the gap between research models and everyday clinical practice.

In summary, this study establishes that subtle but consistent abnormalities in background EEG rhythms carry strong diagnostic information for epilepsy. By leveraging advanced signal processing and machine learning, we present a scalable, non-invasive, and physiology-driven approach that holds significant promise for improving early detection and accessibility of epilepsy diagnosis, particularly in settings where prolonged EEG monitoring is not feasible.

Credit Author Statement

Conceptualization, Albina V. Lebedeva, Tatiana A. Levanova and Alexander N. Pisarchik;

Methodology, Anton E. Malkov, Albina V. Lebedeva, Svetlana A. Gerasimova, Tatiana A. Levanova and Lev A. Smirnov;

Software, Anton E. Malkov, Tatiana A. Levanova, Lev A. Smirnov and Artem A. Sharkov;

Validation, Anton E. Malkov and Tatiana A. Levanova;

Formal analysis, Anton E. Malkov, Svetlana A. Gerasimova, Tatiana A. Levanova, Lev A. Smirnov and Artem A. Sharkov;

Investigation, Anton E. Malkov, Albina V. Lebedeva, Svetlana A. Gerasimova, Tatiana A. Levanova, Lev A. Smirnov, Artem A. Sharkov and Alexander N. Pisarchik;

Data curation, Artem A. Sharkov;

Visualization, Albina V. Lebedeva and Svetlana A. Gerasimova; Supervision, Alexander N. Pisarchik;

Writing – original draft, Anton E. Malkov;

Writing – review & editing, all authors.

Declaration of interests

The authors declare that they have no known competing financial interests or personal relationships that could have appeared to influence the work reported in this paper.

Acknowledgment

This work was supported by the Ministry of Economic Development of the Russian Federation (grant No. 139-15-2025-004 dated 17.04.2025, agreement identifier 000000Ц313925Р3Х 0002).

References

[1] M. H. Fischer, H. Lowenbach, Aktionsstrome des zentralnervensystems unter der einwikung von krampfgiften. i. miteilung strychnine und pickrotoxin, Archiv fur Experimentelle Pathologie und Pharmakologie 174 (1934) 357–382.

[2] S. J. J. Jui, R. C. Deo, P. D. Barua, A. Devi, J. Soar, U. R. Acharya, Application of entropy for automated detection of neurological disorders with electroencephalogram signals: A review of the last decade (2012–2022), IEEE Access 11 (2023) 71905–71924.

[3] A. N. Pisarchik, V. Grubov, V. Maksimenko, et al., Extreme events in epileptic EEG of rodents after ischemic stroke, Eur. Phys. J. Spec. Top. 227 (2018) 921–932.

[4] N. S. Frolov, V. V. Grubov, V. A. Maksimenko, et al., Statistical properties and predictability of extreme epileptic events, Sci. Rep. 9 (1) (2018) 7243.

[5] J. J. Engel, et al., Epilepsy biomarkers, Epilepsia 54 (4) (2013) 61–69.

[6] N. Lai, Z. Li, C. Xu, Y. Wang, Z. Chen, Diverse nature of interictal oscillations: EEG-based biomarkers in epilepsy, Neurobiol. of Dis. 177 (2023) 105999.

[7] H. Işik, E. Sezer, Diagnosis of epilepsy from electroencephalography signals using multilayer perceptron and Elman artificial neural networks and wavelet transform, J. Med. Syst. 36 (1) (2012) 1–13.

[8] E. Sezer, H. Işik, E. Saracoğlu, Employment and comparison of different artificial neural networks for epilepsy diagnosis from EEG signals, J. Med. Syst. 36 (1) (2012) 347–362.

[9] N. Kane, et al., A revised glossary of terms most commonly used by clinical electroencephalographers and updated proposal for the report format of the EEG findings. revision 2017, Clin. Neurophysiol. Pract. 2 (2017) 170–185.

[10] K. J. Werhahn, E. Hartl, K. Hamann, M. Breimhorst, S. Noachtar, Latency of interictal epileptiform discharges in long-term EEG recordings in epilepsy patients, Seizure 29 (2015) 20–25.

[11] A. Krumholz, Driving issues in epilepsy: Past, present, and future, Epilepsy Curr. 9 (2) (2009) 31–35.

[12] M. M. Oto, The misdiagnosis of epilepsy: Appraising risks and managing uncertainty, Seizure 44 (1) (2017) 143–146.

[13] P. P. Lenck-Santini, L. M. de la Prida, Temporal coordination: A key to understanding cognitive and behavioral deficits in epilepsy, in: Epilepsy: A Comprehensive Textbook, Wolters Kluwer, 2022, pp. 114–130.

[14] A. Bragin, L. Li, J. Almajano, C. Alvarado-Rojas, A. Y. Reid, R. J. Staba, J. E. Jr., Pathologic electrographic changes after experimental traumatic brain injury, Epilepsia 57 (5) (2016) 735–745.

[15] N. Roehri, F. Pizzo, F. Bartolomei, F. F. Wendling, C. G. Bénar, What are the assets and weaknesses of HFO detectors? a benchmark framework based on realistic simulations, Plos One 12 (2017) 1–20.

[16] T. L. Babb, J. P. Lieb, W. J. Brown, J. Pretorius, P. H. Crandall, Distribution of pyramidal cell density and hyperexcitability in the epileptic human hippocampal formation, Epilepsia 25 (6) (1984) 721–728.

[17] M. Boly, et al., Altered sleep homeostasis correlates with cognitive impairment in patients with focal epilepsy, Brain 140 (4) (2017) 1026–1040.

[18] X. Li, Y. Hou, Y. Ren, X. Tian, Y. Song, Alterations of theta oscillation in executive control in temporal lobe epilepsy patients, Epilepsy Res. 140 (2018) 148–154.

[19] Y. Sato, A. Ochi, T. Mizutani, H. Otsubo, Low entropy of interictal gamma oscillations is a biomarker of the seizure onset zone in focal cortical dysplasia type II, Epilepsy & Behav. 96 (2019) 155–159.

[20] J. Pyrzowski, M. Siemiński, A. Sarnowska, J. Jedrzejczak, W. M. Nyka, Interval analysis of interictal EEG: Pathology of the alpha rhythm in focal epilepsy, Sci. Rep. 5 (2015) 16230.

[21] M. Panagiotopoulou, C. A. Papasavvas, G. M. Schroeder, R. H. Thomas, P. N. Taylor, Y. Wang, Fluctuations in EEG band power at subject-specific timescales over minutes to days explain changes in seizure evolutions, Hum. Brain Mapp. 43 (8) (2022) 2460–2477.

[22] P. N. Taylor, et al., Normative brain mapping of interictal intracranial EEG to localize epileptogenic tissue, Brain 145 (3) (2022) 939–949.

[23] G. P. Kalamangalam, L. Cara, N. Tandon, An interictal EEG spectral metric for temporal lobe epilepsy lateralization, Epilepsy Res. 108 (10) (2014) 1748–1757.

[24] R. Gao, E. J. Peterson, B. Voytek, Inferring synaptic excitation/inhibition balance from field potentials, NeuroImage 158 (2017) 70–78.

[25] W. T. Kerr, et al., Automated diagnosis of epilepsy using EEG power spectrum, Epilepsia 53 (11) (2012) e189–e192.

[26] M. Amiri, B. Frauscher, J. Gotman, Phase-amplitude coupling is elevated in deep sleep and in the onset zone of focal epileptic seizures, Front. Hum. Neurosci. 10 (2016) 387.

[27] A. Malkov, L. Shevkova, A. Latyshkova, V. Kitchigina, Theta and gamma hippocampal-neocortical oscillations during the episodic-like memory test: Impairment in epileptogenic rats, Exp. Neurol. 354 (2022) 114110.

[28] H. Ma, Z. Wang, C. Li, J. Chen, Y. Wang, Phase-amplitude coupling and epileptogenic zone localization of frontal epilepsy based on intracranial EEG, Front. Neurol. 12 (2021) 718683.

[29] Y. Miao, Y. Iimura, H. Sugano, K. Fukumori, T. Tanaka, Seizure onset zone identification using phase-amplitude coupling and multiple machine learning approaches for interictal electrocorticogram, Cogn. Neurodyn. 17 (6) (2023) 1591–1607.

[30] V. Grigorovsky, et al., Delta-gamma phase-amplitude coupling as a biomarker of postictal generalized EEG suppression, Brain Commun. 2 (2) (2020) fcaa182.

[31] P. Fries, Rhythms for cognition: Communication through coherence, Neuron 88 (1) (2015) 220–235.

[32] M. M. Elkholy, Disruption of EEG resting state functional connectivity in patients with focal epilepsy, Egypt. J. Neurol. Psychiatr. Neurosurg. 59 (2023) 122.

[33] M. Takigawa, G. Wang, H. Kawasaki, H. Fukuzako, EEG analysis of epilepsy by directed coherence method: A data processing approach, Int. J. Psychophysiol. 21 (2–3) (1996) 65–73.

[34] L. N. Nerobkova, et al., The study of electrophysiological mechanisms of pathological system regression among patients with epilepsy by the method of spectral-coherence analysis and the method of dipole sources, Epilepsy Paroxysm. Condit. 5 (1) (2013) 22–30.

[35] A. Coito, et al., Altered directed functional connectivity in temporal lobe epilepsy in the absence of interictal spikes: A high-density EEG study, Epilepsia 57 (3) (2016) 402–411.

[36] M. Carboni, et al., Abnormal directed connectivity of resting state networks in focal epilepsy, NeuroImage: Clinical 27 (2020) 102336.

[37] X. Jiang, X. Liu, Y. Liu, Q. Wang, B. Li, L. Zhang, Epileptic seizures detection and the analysis of optimal seizure prediction horizon based on frequency and phase analysis, Front. Neurosci. 17 (2023) 1191683.

[38] A. Stoller, Slowing of the alpha-rhythm of the electroencephalogram and its association with mental deterioration and epilepsy, J. Mental Sci. 95 (401) (1949) 971–984.

[39] E. Santiago-Rodriguez, T. Harmony, L. Cárdenas-Morales, A. Hernández, Analysis of background EEG activity in patients with juvenile myoclonic epilepsy, Seizure 17 (5) (2008) 437–445.

[40] R. J. Staba, G. A. Worrell, What is the importance of abnormal "background" activity in seizure generation?, in: H. Scharfman, P. Buckmaster (Eds.), Issues in Clinical Epileptology: A View from the Bench, Vol. 813, Springer, 2014, pp. 15–26.

[41] M. Lancel, Cortical and subcortical EEG in relation to sleep-wake behavior in mammalian species, Neuropsychobiology 28 (3) (1992) 154–159.

[42] D. J. Dijk, D. P. Brunner, A. A. Borbély, Time course of EEG power density during long sleep in humans, Am. J. Physiol. 258 (3) (1990) R650–R661.

[43] C. E. Châtillon, C. G. Bénar, C. Grova, J. Gotman, MEG reveals widespread interictal delta and theta activity in focal epilepsy, Epilepsia 63 (5) (2022) 1189–1201.

[44] Y. Tanoue, et al., Specific oscillatory power changes and their efficacy for determining laterality in mesial temporal lobe epilepsy: A magnetoencephalographic study, Front. Neurology 12 (2021) 617291.

[45] B. Clemens, Pathological theta oscillations in idiopathic generalized epilepsy, Clin. Neurophysiol. 115 (6) (2004) 1436–1441.

[46] J. Sarnthein, A. Morel, A. von Stein, D. Jeanmonod, Thalamocortical theta coherence in neurological patients at rest and during a working memory task, Int. J. Psychophysiol. 57 (2) (2005) 87–96.

[47] O. N. Arski, J. M. Young, M. L. Smith, G. M. Ibrahim, The oscillatory basis of working memory function and dysfunction in epilepsy, Front. Hum. Neurosci. 14 (2021) 387.

[48] C. Helmstaedter, C. E. Elger, Cognitive consequences of epilepsy: Persistence, determinants, and treatment possibilities, Epilepsy & Behavior 4 (S2) (2003) 55–67.

[49] Ö. Yildirim, U. B. Baloglu, U. R. Acharya, A deep convolutional neural network model for automated identification of abnormal EEG signals, Neural Comput. Appl. 32 (2020) 15857–15868.

[50] C. H. L. Hinchliffe, M. Yogarajah, S. Elkommos, H. Tang, D. Abasolo, Nonictal electroencephalographic measures for the diagnosis of functional seizures, Epilepsia 65 (11) (2024) 3293–3302.

[51] P. Myers, et al., Diagnosing epilepsy with normal interictal EEG using dynamic network models, Ann. Neurol. 97 (5) (2025) 907–918.